Vector cavity optomechanics in the parameter configuration of optomechanically induced transparency

Hao Xiong,* Ya-Min Huang, Liang-Liang Wan, and Ying Wu†
School of Physics, Huazhong University of Science and Technology, Wuhan 430074, People's Republic of China
(Received 22 January 2016; published 8 July 2016)

We propose the concept of vector cavity optomechanics in which the polarization behavior of light fields is introduced to achieve optomechanical control. The steady states and optomechanically induced transparency are studied in the vector regime, and we show that the polarization of optical fields may be a powerful tool to identify the underlying physical process and control the signal of optomechanically induced transparency. In particular, the conditions for obtaining a linearly polarized output probe field is given, which reveal some nontrivial polarizing effects. Despite its conceptual simplicity, vector cavity optomechanics may entail a wide range of intriguing phenomena and uncover a novel understanding for optomechanical interaction.

DOI: 10.1103/PhysRevA.94.013816

I. INTRODUCTION

A typical optomechanical system consists of a Fabry-Pérot cavity in which one mirror of the cavity is movable as a mechanical resonator [1]. The photons inside the cavity can exert forces on the movable mirror and consequently change the position of the mirror. Meanwhile, the dynamical behavior of the cavity fields depends sensitively on the position of the mirror [2]. Such a feedback backaction mechanism enables external optical control of both the mechanical motion and the light transmission [3–5]. Cavity optomechanics, which describes the radiation pressure interaction between well-coupled optical modes and mechanical oscillations, has progressed enormously in recent years and plays an important role in various fields of physics, including precision measurements [6–8], frequency comb generation [9–11], asymmetric optical transmission [12,13], slowing and storage of light pulses [14,15], squeezing of light and nanomechanical motion [16], and even fundamental tests of quantum mechanics [17]. These achievements provide unprecedented access to a new type of light-matter interface and enable a new class of devices in on-chip sensing and signal processing.

Although most research has concentrated on achieving optomechanical control through scalar optical fields (that is the optical fields are described by the parameters frequency, amplitude, and phase), the polarization behavior, which describes the vector nature of light fields, however, has not been well discussed in optomechanical systems. In some previous works, optomechanical systems with bidimensional dynamical backaction (where the mechanical motion is described by a vector field) have been experimentally realized, and the dynamical effects reveal a novel topological instability which underlies the remarkable nonconservative nature of the optomechanical interaction [18].

Optical modulation by means of polarization management plays a relevant role in coherent optical communications, gyroscopes, and sensors [19,20]. In this paper, we introduce a group of orthogonal basis vectors of polarization in an optomechanical system and consider that the optomechanical system is driven by linearly polarized fields. Such a general approach can be applied to various configurations and regimes of interest, but here we focus on the parameter configuration of optomechanically induced transparency in the weak-coupling regime. We show that rich nontrivial behaviors occur if the vector nature of the light field is introduced into the topic of cavity optomechanics. Discussion of optomechanically induced transparency in the vector regime reveals that the polarization of the optical fields may be a powerful tool to identify the underlying physical process and control the signal of optomechanically induced transparency. The conditions of obtaining a linearly polarized output probe field are discussed, which reveal a nontrivial optomechanical polarizer obeys Malus' law in the parameter configuration of optomechanically induced transparency.

This paper is organized as follows. We give a description of the vector optomechanical system in Sec. II where a group of orthogonal basis vectors of polarization in an optomechanical system is introduced and the optomechanical system is driven by linearly polarized fields. In Sec. III, we discuss the features of optomechanically induced transparency in the vector regime, including the steady state and the output field. In Sec. IV, the conditions of obtaining a linearly polarized output probe field are discussed, and we find a nontrivial polarizing effect—an optomechanical polarizer. Finally, a conclusion of the results is summarized in Sec. V.

II. DESCRIPTION OF THE VECTOR OPTOMECHANICAL SYSTEM

Figure 1(a) gives the schematic of a vector optomechanical system, which consists of a Fabry-Pérot cavity with one movable mirror. The mass of the movable mirror is m, and the eigenfrequency is Ω_m. For the Fabry-Pérot cavity, a group of orthogonal basis vectors of polarization $(\vec{e}_\updownarrow,\vec{e}_\leftrightarrow)$ corresponding to TE and TM modes can be introduced, and any linearly polarized field with polarization vector $\vec{e}$ can be decomposed as $\vec{e} = \alpha\vec{e}_\updownarrow + \beta\vec{e}_\leftrightarrow$ with $|\alpha|^2 + |\beta|^2 = 1$ [shown in Fig. 1(b)]. In the present case, the orthogonal bases $\updownarrow$ and $\leftrightarrow$ are not special but are chosen for simplicity. The orthogonal basis vectors of polarization corresponding to TE and TM modes

*haoxiong1217@gmail.com
†yingwu2@126.com

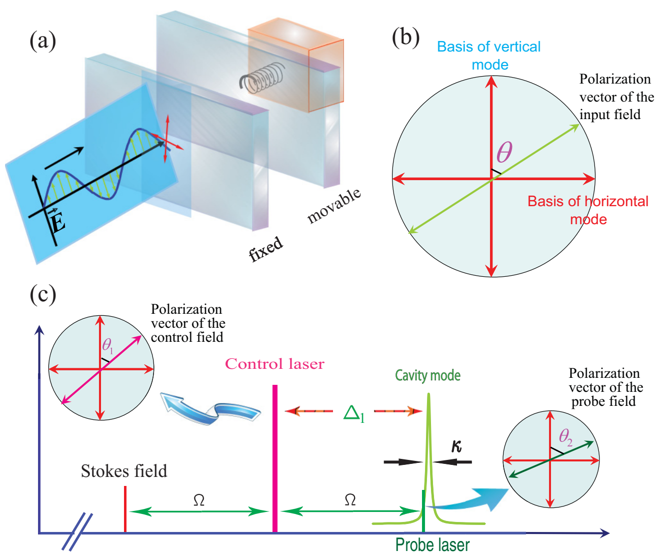

FIG. 1. (a) Schematic of a vector optomechanical system. (b) Any linearly polarized field with polarization vector $\vec{e}$ can be decomposed by a group of orthogonal basis vectors of polarization in the vector optomechanical system. (c) Frequency spectrogram of a vector optomechanical system in the parameter configuration of optomechanically induced transparency. Here both control and probe fields are linearly polarized optical fields, and the included angle between the polarization of control (probe) field and the vertical mode is θ_1 (θ_2). The cavity resonance frequency ω_c which has a linewidth of κ is detuned by Δ_1 from the control field.

may be introduced similarly for other types of cavity or resonator, and some previous works on a ring resonator [21] have experimentally demonstrated the effect of the polarization rotation induced by curved waveguides.

The interaction between light and these nano- or micromechanical systems is determined by the form of optomechanical coupling, and the nonrelativistic Hamiltonian of the interaction between cavity fields and a moving mirror via radiation pressure can be derived from the wave equation with time-varying boundary conditions [22]. As depicted in Figs. 1(a) and 1(b), an optomechanical system driven by vector optical fields can be described by the following Hamiltonian:

$$\hat{H} = \hat{H}_0 + \hbar G\hat{x} \sum_{j=\updownarrow,\leftrightarrow} \hat{a}_j^\dagger \hat{a}_j + i\hbar\sqrt{\eta\kappa} \sum_{j=\updownarrow,\leftrightarrow} (\hat{a}_j^\dagger S_j - \hat{a}_j S_j^*),$$
$$\hat{H}_0 = \frac{\hat{p}^2}{2m} + \frac{m\Omega_m^2 \hat{x}^2}{2} + \hbar\omega_c \sum_{j=\updownarrow,\leftrightarrow} \hat{a}_j^\dagger \hat{a}_j, \tag{1}$$

where $\hat{p}$ and $\hat{x}$ are the momentum and position operators of the mechanical resonator, respectively. $\hat{a}_j$ ($\hat{a}_j^\dagger$) are the annihilation (creation) operators of the orthogonal cavity modes with degenerate cavity resonance frequency ω_c. G is the optomechanical coupling constant for both orthogonal cavity modes. κ is the total loss rate of the cavity field which contains an intrinsic loss rate κ_0 and an external loss rate κ_{ex}. The coupling parameter $\eta = \kappa_{\text{ex}}/\kappa$, which describes the coupling between pump and cavity fields, can be continuously adjusted. S_j is the amplitudes of the driving fields. For linearly polarized input fields $\sum_k \vec{e}_k s_k e^{-i\omega_k t}$, where $s_k = e^{-i\theta_k}\sqrt{P_k/\hbar\omega_k}$ is the amplitude of the kth input field normalized to a photon flux at the input of the cavity with P_k as the power of the kth input field, $\vec{e}_k$ is the unit vector of polarization of the kth input field and can be represented as $\vec{e}_k = e_{k\updownarrow} \updownarrow + e_{k\leftrightarrow} \leftrightarrow$ with $e_{k\updownarrow}$ and $e_{k\leftrightarrow}$ as the projections of $\vec{e}_k$ onto the vertical and horizontal modes, respectively. Using the included angle θ_k between $\vec{e}_k$ and the vertical mode as shown in Fig. 1(b), we obtain $e_{k\updownarrow} = \cos\theta_k$ and $e_{k\leftrightarrow} = \sin\theta_k$. So $S_\updownarrow = \sum_k s_k \cos\theta_k e^{-i\omega_k t}$, $S_\leftrightarrow = \sum_k s_k \sin\theta_k e^{-i\omega_k t}$.

III. OPTOMECHANICALLY INDUCED TRANSPARENCY IN THE VECTOR REGIME

It has been demonstrated that electromagnetically induced transparency, which originally discovered in atomic vapors [23–25], has an analog in the optomechanical system through mechanical effects of light [26–31]. In the parameter configuration of optomechanically induced transparency [14], the optomechanical system is driven by two fields: a strong control field with amplitude s_1 and frequency ω_1 and a weak probe field with amplitude s_2 and frequency ω_2. In the present paper, we consider that both control and probe fields are linearly polarized optical fields [shown in Fig. 1(c)], and the included angle between the polarization of control (probe) field and the vertical mode is θ_1 (θ_2).

Based on the Hamiltonian, Heisenberg-Langevin equations can be obtained to describe the evolution of the cavity fields and the properties of the mechanical motion of the moving mirror [32]. In this paper, we are interested in the mean response of the vector optomechanical system, so the operators can be reduced to their expectation values in the weak-coupling regime (the mean-field approximation of factorizing averages, viz. $\langle Qc\rangle = \langle Q\rangle\langle c\rangle$ is also used), and the Heisenberg-Langevin equations reduced to a group of nonlinear evolution equations (in a frame rotating at ω_1) [26] are as follows:

$$\begin{aligned} \dot{a}_\updownarrow &= (i\Delta_1 - iGx - \kappa/2)a_\updownarrow + \sqrt{\eta\kappa}(s_1\cos\theta_1 \\ &\quad + s_2\cos\theta_2 e^{-i\Omega t}), \\ \dot{a}_\leftrightarrow &= (i\Delta_1 - iGx - \kappa/2)a_\leftrightarrow \\ &\quad + \sqrt{\eta\kappa}(s_1\sin\theta_1 + s_2\sin\theta_2 e^{-i\Omega t}), \\ \ddot{x} + \Gamma_m\dot{x} + \Omega_m^2 x &= -\frac{\hbar G}{m}\sum_{j=\updownarrow,\leftrightarrow} a_j^* a_j, \end{aligned} \tag{2}$$

where $\Delta_1 = \omega_1 - \omega_c$, $\Omega = \omega_2 - \omega_1$, the quantum and thermal noise terms are dropped, and the decay rates of the mechanical oscillator (Γ_m) are introduced classically.

It would be advantageous to choose as a reference the polarization of the control field, viz. $\theta_1 = 0$, because the problem is clearly rotationally invariant. In this case, the above equations can be linearized for the case of $|s_2| \ll |s_1|$ [33], and the solution can be written as $a_\updownarrow = \bar{a}_\updownarrow + \delta a_\updownarrow$, $a_\leftrightarrow = A_\leftrightarrow^- e^{-i\Omega t} + A_\leftrightarrow^+ e^{i\Omega t}$, $x = \bar{x} + \delta x$, where $\bar{a}_\updownarrow = -\sqrt{\eta\kappa} s_1 \wp$ as well as $\bar{x} = -\hbar G\eta\kappa|s_1\wp|^2/m\Omega_m^2$ are the steady-state solutions and $\delta a_\updownarrow = A_\updownarrow^- e^{-i\Omega t} + A_\updownarrow^+ e^{i\Omega t}$ as well as

$\delta x = Xe^{-i\Omega t} + X^* e^{i\Omega t}$ are the linearized perturbations with

$$A_{\updownarrow}^{+} = \frac{-iG\sqrt{\eta\kappa}s_1\wp X^*}{\varpi(\Delta_1,-\Omega)}, \qquad A_{\leftrightarrow}^{+} = 0,$$
$$A_{\updownarrow}^{-} = \frac{iG\bar{a}_{\updownarrow}X - \sqrt{\eta\kappa}s_2\cos\theta_2}{\varpi(\Delta_1,\Omega)},$$
$$A_{\leftrightarrow}^{-} = \frac{iG\bar{a}_{\leftrightarrow}X - \sqrt{\eta\kappa}s_2\sin\theta_2}{\varpi(\Delta_1,\Omega)},$$
$$X = -\frac{\alpha_0\eta\kappa\wp^* s_1^* s_2\cos\theta_2}{\varpi(\Delta_1,\Omega)[\theta(\Omega) + i\alpha_0 G\eta\kappa A(\Delta_1,\Omega)|s_1\wp|^2]},$$

$\wp = 1/(i\Delta_1 - iG\bar{x} - \kappa/2)$, $A(\Delta_1,\Omega) = -2i(\Delta_1 - G\bar{x})/\{\varpi(\Delta_1,\Omega)[\varpi(\Delta_1,-\Omega)]^*\}$, $\alpha_0 = \hbar G/m$, $\varpi(x,y) = ix + iy - iG\bar{x} - \kappa/2$, and $\theta(x) = \Omega_m^2 - x^2 - i\Gamma_m x$. From the solution we note a special situation: $X = A_{\updownarrow}^{+} = 0$ when $\theta_2 = \pi/2$. In this case, although both control and probe fields are incident upon the optomechanical system, the oscillator and the fields are in a steady state with $x = \bar{x}$ which depends on the intensity of the control field only.

In what follows, we will give some discussion on the output field. The output field of the optomechanical system can be obtained by using the input-output relation $s_{\text{out}} = s_{\text{in}} - \sqrt{\eta\kappa}a$. In the linearized regime, the output field contains a frequency component of $\omega_1 - \Omega$ (Stokes field), a frequency component at control field ω_1, and a frequency component at probe field ω_2.

From the linearized solution, the Stokes field is always linearly polarized due to the relation $\arg(A_{\updownarrow}^{+}) = \arg(A_{\leftrightarrow}^{+})$. The polarization vector of the Stokes field is (1,0), which clearly turns out that the Stokes field has the same polarization with the control field. Such a result identifies the conversion path of the Stokes field in the linearized regime: The Stokes field originates from the down-conversion of the control field [34], which also implies that the polarization of the output field may be a powerful tool to identify the underlying physical process. The intensity of the Stokes field can be obtained as follows:

$$I_{\text{Stokes}} = \eta\kappa G^2|s_1|^2\left|\frac{\wp X^*}{\varpi(\Delta_1,-\Omega)}\right|^2 \propto \cos^2\theta_2, \tag{3}$$

which is determined by the angle between the polarizations of the control and probe fields and vanish for orthogonal cases.

The output field at the frequency of the control field is also always linearly polarized with the polarization vector (1,0). The intensity of the output field at the frequency of the control field can be obtained as $|s_1|^2|1 + \eta\kappa\wp|^2$, which is independent of the polarizations of the control and probe fields. The output field at the frequency of the probe field is of great interest, and we obtain the field as

$$s_{\text{out}}(\omega_2) = s_2\cos\theta_2(\Phi_2 - \Phi_1)\updownarrow + s_2\sin\theta_2\Phi_2 \leftrightarrow, \tag{4}$$

where

$$\Phi_1 = \frac{\eta\kappa}{\varpi^2(\Delta_1,\Omega)[A(\Delta_1,\Omega) + B(\Delta_1,\Omega)]},$$
$$\Phi_2 = 1 + \frac{\eta\kappa}{\varpi(\Delta_1,\Omega)}, \quad B(\Delta_1,\Omega) = \frac{\theta(\Omega)}{i\alpha_0 G\eta\kappa|\wp s_1|^2}. \tag{5}$$

In general, the output field at the frequency of the probe field is elliptical polarized instead of linearly polarized. The physical interpretation is that there are two sources (or paths) for the output field at the frequency of the probe field: One is the input field of the probe field, and the other is the up-conversion of the control field. The superposition of the two sources with different polarizations leads to the elliptical polarized field. In the conventional optomechanical system, both the control and probe fields are of the same polarization, and the coherent superposition of the two sources results in the phenomenon of optomechanically induced transparency.

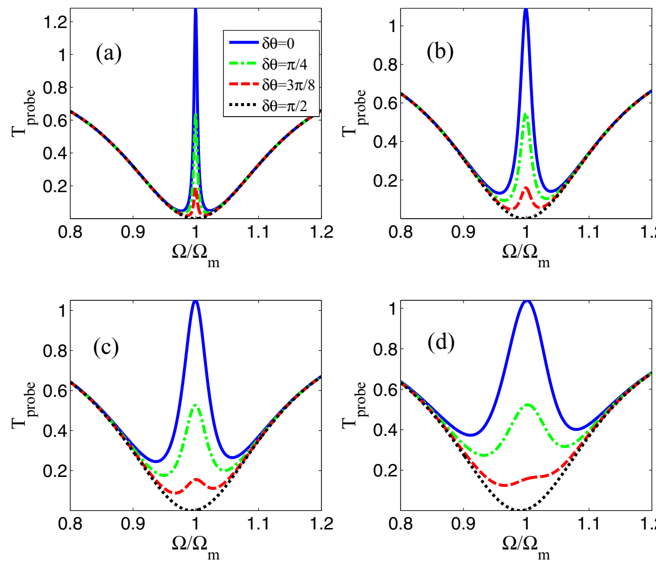

FIG. 2. The transmission of probe fields with different polarization versus Ω under control fields with different powers: (a) 1 mW, (b) 3 mW, (c) 6 mW, and (d) 10 mW. The wavelength of the control field is 532 nm, $\delta\theta = \theta_1 - \theta_2$, and the parameters used in the calculation are chosen from the recent experiment [26]: $m = 20$ ng, $G/2\pi = -12$ GHz/nm, $\eta = 1/2$, $\Gamma_m/2\pi = 41.0$ kHz, $\kappa/2\pi = 15.0$ MHz, $\Omega_m/2\pi = 51.8$ MHz, and $\Delta_1 = -\Omega_m$.

The transmission of the probe field in the vector optomechanical system can be obtained as

$$T_{\text{probe}} = |\Phi_2|^2 + |\Phi_1|^2\cos^2\theta_2, \tag{6}$$

which reveals optomechanically induced transparency in the vector regime. By tuning the polarizations of the probe field, the transmission of the probe field changes periodically. The transmission of probe fields with different polarizations is shown in Fig. 2 where conventional optomechanically induced transparency occur when $\delta\theta = 0$ whereas the signal of optomechanically induced transparency vanishes for the orthogonal case in which the optomechanical system falls into the steady state. It is interesting that the coherent phenomenon (the signal of optomechanically induced transparency) disappears if the two source paths of the output field at the frequency of the probe field are completely identified by the polarization.

IV. OPTOMECHANICAL POLARIZER

The transmission of the probe field depends on functions $|\Phi_1|$ and $|\Phi_2|$. As shown in Fig. 3, as the power of the control field increases, the raised peak of the function $|\Phi_1|$ becomes wider obviously, which is responsible for the broadening of the

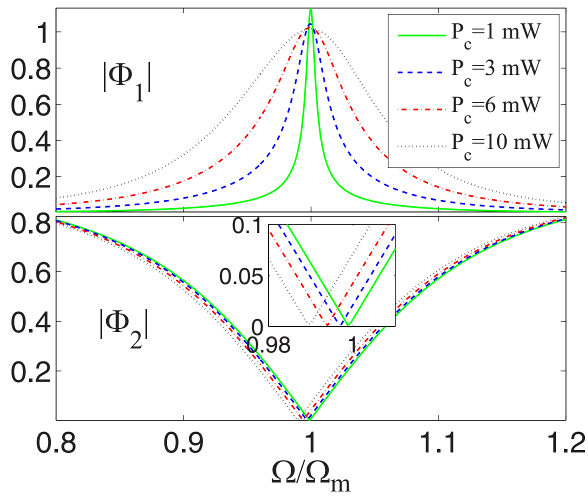

FIG. 3. Calculation results of $|\Phi_1|$ and $|\Phi_2|$ versus Ω in the parameter configuration of optomechanically induced transparency.

induced transparency, whereas the function $|\Phi_2|$ only shifts tinily due to the modification of the cavity length.

As we have shown, the output field at the frequency of the probe field is elliptically polarized instead of linearly polarized in general. The conditions of obtaining a linearly polarized output probe field are quite interesting. From the expression (4) which describes the output field at the frequency of the probe field, we can directly obtain that the output field $s_{\rm out}(\omega_2)$ is linearly polarized if $\theta_2 = \pi/2$ or $\theta_2 = 0$. The former is the orthogonal case in which the optomechanical system falls into the steady state, whereas the latter is conventional optomechanically induced transparency. These two conditions are trivial for obtaining a linearly polarized output probe field via optomechanical interaction.

A nontrivial condition of obtaining a linearly polarized output probe field can exist for the critical coupling case of $\eta = 1/2$. Figure 3 shows that Φ_2 achieves a zero point near $\Omega = \Omega_m$ [35]. Analytically, if the parameters of the optomechanical system satisfy the condition $\Delta_1 - G\bar{x} = -\Omega$ [36], then we have $\Phi_2 = 0$, and the output probe field reduces to $-s_2\Phi_1 \cos\theta_2 \updownarrow$, which is obviously a linearly polarized field with the same polarization of the control field, and the intensity $I_{\rm probe} = |s_2\Phi_1|^2 \cos^2 \delta\theta$ obeys Malus' law. We call this phenomenon an optomechanical polarizer. In contrast to conventional bulk polarizers [19,20], an optomechanical polarizer can be adjusted rapidly by tuning the polarization of the control field.

V. CONCLUSIONS

We study the vector cavity optomechanics in the parameter configuration of optomechanically induced transparency. The steady states and optomechanically induced transparency are studied in the vector regime, and we show that the polarization of the optical fields may be a powerful tool to identify the underlying physical process and control the signal of optomechanically induced transparency. Despite its conceptual simplicity, vector cavity optomechanics may entail a wide range of intriguing phenomena and uncover a novel understanding for optomechanical interaction. In the present paper, we only focus on the case that the input fields are linearly polarized optical fields. The input fields with other polarization states, such as circular polarization and the Bessel beam, may give rise to rich interesting effects due to the angular momentum carried in the light. A non-Abelian synthetic gauge field (spin-orbit coupling) in a vector cavity optomechanical array, which is a natural continuation of the implementation of topological phases of sound and light based on cavity optomechanics [37], is also an exciting perspective.

ACKNOWLEDGMENTS

The work was supported by the National Basic Research Program of China (Grant No. 2016YFA0301200), the National Fundamental Research Program of China (Grant No. 2012CB922103), and the National Science Foundation (NSF) of China (Grants No. 11375067, No. 11275074, No. 11374116, No. 11405061, and No. 11574104).

[1] M. Aspelmeyer, T. J. Kippenberg, and F. Marquardt, Cavity optomechanics, Rev. Mod. Phys. **86**, 1391 (2014).

[2] H. Xiong, L.-G. Si, X. Lü, X.-X. Yang, and Y. Wu, Review of cavity optomechanics in the weak-coupling regime: from linearization to intrinsic nonlinear interactions, Sci. China: Phys., Mech. Astron. **58**, 1 (2015).

[3] B. P. Hou, L. F. Wei, and S. J. Wang, Optomechanically induced transparency and absorption in hybridized optomechanical systems, Phys. Rev. A **92**, 033829 (2015).

[4] Q. Wu, J. Q. Zhang, J. H. Wu, M. Feng, and Z. M. Zhang, Tunable multi-channel inverse optomechanically induced transparency and its applications, Opt. Express **23**, 18534 (2015).

[5] P. C. Ma, J. Q. Zhang, Y. Xiao, M. Feng, and Z. M. Zhang, Tunable double optomechanically induced transparency in an optomechanical system, Phys. Rev. A **90**, 043825 (2014).

[6] J. D. Teufel *et al.*, Nanomechanical motion measured with an imprecision below that at the standard quantum limit, Nat. Nanotechnol. **4**, 820 (2009).

[7] E. Gavartin, P. Verlot, and T. J. Kippenberg, A hybrid on-chip optomechanical transducer for ultrasensitive force measurements, Nat. Nanotechnol. **7**, 509 (2012).

[8] W. He, J. J. Li, and K. D. Zhu, Coupling-rate determination based on radiation-pressure-induced normal mode splitting in cavity optomechanical systems, Opt. Lett. **35**, 339 (2010).

[9] P. Del'Haye *et al.* Optical frequency comb generation from a monolithic microresonator, Nature (London) **450**, 1214 (2007).

[10] H. Xiong, L.-G. Si, X.-Y. Lü, X. Yang, and Y. Wu, Carrier-envelope phase-dependent effect of high-order sideband generation in ultrafast driven optomechanical system, Opt. Lett. **38**, 353 (2013); Nanosecond-pulse-controlled higher-order

sideband comb in a GaAs optomechanical disk resonator in the non-perturbative regime, Ann. Phys. (N.Y.) **349**, 43 (2014).
[11] C. Cao *et al.*, Tunable high-order sideband spectra generation using a photonic molecule optomechanical system, Sci. Rep. **6**, 22920 (2016).
[12] X.-W. Xu and Y. Li, Optical nonreciprocity and optomechanical circulator in three-mode optomechanical systems, Phys. Rev. A **91**, 053854 (2015); H. Xiong, L.-G. Si, X. Yang, and Y. Wu, Asymmetric optical transmission in an optomechanical array, Appl. Phys. Lett. **107**, 091116 (2015).
[13] B. Peng *et al.*, Parity—time-symmetric whispering-gallery microcavities, Nat. Phys. **10**, 394 (2014).
[14] A. H. Safavi-Naeini *et al.*, Electromagnetically induced transparency and slow light with optomechanics, Nature (London) **472**, 69 (2011).
[15] Y. Jiao, H. Lü, J. Qian, Y. Li, and H. Jing, Amplifying higher-order sidebands in optomechanical transparency with gain and loss, arXiv:1602.05308.
[16] A. H. Safavi-Naeini *et al.*, Squeezed light from a silicon micromechanical resonator, Nature (London) **500**, 185 (2013).
[17] I. Pikovski, M. R. Vanner, M. Aspelmeyer, M. S. Kim, and C. Brukner, Probing Planck-scale physics with quantum optics, Nat. Phys. **8**, 393 (2012).
[18] A. Gloppe, P. Verlot, E. Dupont-Ferrier, A. Siria, P. Poncharal, G. Bachelier, P. Vincent, and O. Arcizet, Bidimensional nano-optomechanics and topological backaction in a non-conservative radiation force field, Nat. Nanotechnol. **9**, 920 (2014).
[19] J. N. Damask, Polarization Optics in Telecommunications, *Polarization Optics in Telecommunications* (Springer, New York, 2004).
[20] V. V. Tuchin, L. V. Wang, and D. A. Zimnyakov, Optical Polarization in Biomedical Applications, *Optical Polarization in Biomedical Applications* (Springer, New York, 2006).
[21] A. Melloni, F. Morichetti, and M. Martinelli, Polarization conversion in ring resonator phase shifters, Opt. Lett. **29**, 2785 (2004).
[22] C. K. Law, Interaction between a moving mirror and radiation pressure: A Hamiltonian formulation, Phys. Rev. A **51**, 2537 (1995).
[23] M. Fleischhauer, A. Imamoglu, and J. P. Marangos, Electromagnetically induced transparency: Optics in coherent media, Rev. Mod. Phys. **77**, 633 (2005).
[24] M. Mücke *et al.*, Electromagnetically induced transparency with single atoms in a cavity, Nature (London) **465**, 755 (2010).
[25] W.-X. Yang, A.-X. Chen, L.-G. Si, K. Jiang, X. Yang, and R.-K. Lee, Three coupled ultraslow temporal solitons in a five-level tripod atomic system, Phys. Rev. A **81**, 023814 (2010).
[26] S. Weis *et al.*, Optomechanically induced transparency, Science **330**, 1520 (2010).
[27] G. S. Agarwal and S. Huang, Electromagnetically induced transparency in mechanical effects of light, Phys. Rev. A **81**, 041803 (2010).
[28] H. Wang, X. Gu, Y.-x. Liu, A. Miranowicz, and F. Nori, Optomechanical analog of two-color electromagnetically induced transparency: Photon transmission through an optomechanical device with a two-level system, Phys. Rev. A **90**, 023817 (2014).
[29] F. C. Lei, M. Gao, C. Du, Q. L. Jing, and G. L. Long, Three-pathway electromagnetically induced transparency in coupled-cavity optomechanical system, Opt. Express **23**, 11508 (2015).
[30] R. J. Xiao, G. X. Pan, and L. Zhou, Analog multicolor electromagnetically induced transparency in multimode quadratic coupling quantum optomechanics, J. Opt. Soc. Am. B **32**, 1399 (2015).
[31] H. Jing *et al.*, Optomechanically-induced transparency in parity-time-symmetric microresonators, Sci. Rep. **5**, 9663 (2015).
[32] X. Lü, H. Jing, J.-Y. Ma, and Y. Wu, PT-Symmetry-Breaking Chaos in Optomechanics, Phys. Rev. Lett. **114**, 253601 (2015).
[33] H. Xiong, L.-G. Si, A.-S. Zheng, X. Yang, and Y. Wu, Higher-order sidebands in optomechanically induced transparency, Phys. Rev. A **86**, 013815 (2012); H. Xiong, L.-G. Si, X.-Y. Lü, and Y. Wu, Optomechanically induced sum sideband generation, Opt. Express **24**, 5773 (2016).
[34] Cavity optomechanics in the vector nonlinear regime is also interesting. The two-photon down-conversion of the probe field also leads to the generation of the Stokes field, which has the same polarization with the probe field. Thus the Stokes field is elliptically polarized instead of linearly polarized if the nonlinear terms of the optomechanical dynamical equations are taken into account, and the polarization of the Stokes field may reveal nonlinear optomechanical interaction in a more robust way.
[35] Here $\Delta_1 = -\Omega_m$ is used in the parameter configuration of optomechanically induced transparency. The underlying condition for Φ_2 achieving zero point is $\Delta_1 \approx -\Omega$.
[36] The expression of Φ_2 can be reduced to $iG\bar{x}/(iG\bar{x} + \kappa/2)$ for the condition $\Delta_1 = -\Omega$. Thus the difference between conditions $\Delta_1 - G\bar{x} = -\Omega$ and $\Delta_1 = -\Omega$ is quite modest due to the fact that $G\bar{x}/\kappa \ll 1$ in the present case.
[37] V. Peano, C. Brendel, M. Schmidt, and F. Marquardt, Topological Phases of Sound and Light, Phys. Rev. X **5**, 031011 (2015).